

Modern Trends in Gamma Detection Systems for Emergency Response

Sanjoy Mukhopadhyay^{*a}, Richard Maurer^a, Paul Guss^b

^aRemote Sensing Laboratory–Andrews AFB, Nevada National Security Site, Andrews Air Force Base, Maryland, USA 20762; ^bRemote Sensing Laboratory–Nellis AFB, Nevada National Security Site, North Las Vegas, Nevada, USA 89030

ABSTRACT

The scope and applicability of detecting gamma-emitting materials by first responders and advanced searchers have changed considerably over the last 15 years. More often than not the searchers are being asked to obtain an image of the gamma sources that are shielded or otherwise inaccessible. They are constantly being tasked to localize a moving source in busy traffic. Commercially available gamma detection units and prototype Government-funded research products use complex techniques such as hybrid imaging processes (combination of traditional Compton imaging with coded aperture masks, for example, modified uniformly redundant array [MURA] patterns). Standalone radiation detection systems are increasingly capitalizing on multi-modal detection, emphasizing on data fusion, informatics, and novel signal/signature exploitations.

At the request of the U.S. Department of Homeland Security (DHS) Countering Weapons of Mass Destruction (CWMD) Office, previously known as the Domestic Nuclear Detection Office (DNDO), a study committee from the American Physical Society has recommended that emphasis is kept on the ability to detect shielded special nuclear material with high sensitivity and reliability. Development of new and improved detection algorithms (e.g., principal component analysis, maximum-likelihood estimation algorithm, and others) has been encouraged. CWMD has been urged to focus on signature identification in its nuclear forensic portfolio. Newer materials like $\text{SrI}_3:\text{Eu}^{2+}$, $\text{LaBr}_3:\text{Ce}$, $\text{CeBr}_3:\text{Ca}^{2+}$ with fast rise time and short decay time of gamma pulses, high intrinsic gamma sensitivity, high gamma energy resolution, and high-efficiency conversion of excitation energy to fluorescent radiation are constantly being sought to build gamma detectors. Neutron detection and associated activation analysis using a gamma ray detection system is highly encouraged.

There is a constant demand for miniaturization of gamma radiation detection system for tactical usage in the field—the most sought-after device must be lightweight, easy to use, should be able to withstand harsh environmental conditions, long shelf life with commensurate long battery life, high sensitivity (with preferably high resolution), capable of creating flexible and configurable alarm conditions with directional sensitivity. This array of technical constraints demands stringent specifications on the readout electronics, data acquisition technologies, interoperability and interconnectivity of data output and strict quality assurance of the detection and measurement devices.

In recent years the CWMD has developed a system called Intelligent Radiation Sensing System (IRSS) that harnesses the information gathered by ubiquitous radiation monitoring systems deployed by the state, local, and tribal law enforcement organizers [1]. The IRSS was created to better equip law enforcement entities to protect large cities from the threats and harmful effects of nuclear or radiological incidents and emergencies. The IRSS uses a breakthrough technology that networks a group of portable radiation detectors with improved detection, localization, and identification of potential radiological threat. The program created a robust, flexible network architecture along with advanced data fusion algorithms that combine information from many detectors.

A study [2] published in the *Journal of Materials Research* summarized the basic requirements for materials to be used in development of scalable radiation detection systems that considered the critical material performance metrics of energy resolution (1% for semiconductors like CZT, <3% for scintillators like $\text{LaBr}_3:\text{Ce}$ at 662 keV primary gamma ray energy from ^{137}Cs isotope), fast timing including high mobility of electrons and holes in the semiconductors and fast scintillation processes, high spatial resolution for imaging purposes, high intrinsic detection efficiency (requiring high density, high effective atomic number Z_{eff}), high geometric efficiency achieved sometimes by occlusion processes, neutron detection efficiency and operational factors like cost, ease of use, use of peripheral equipment like thermomechanical engines to stabilize the detection systems.

Exciting new research and development work utilizing effective data mining algorithms is being performed at universities, national laboratories, and commercial institutions in gamma ray detection technology. For example, gamma ray imaging techniques first used in space telescopes are being applied in modern security and health systems in a joint project between the University of Southampton and industrial partner Symetrica. The project

aims to develop a new coded aperture imaging system that could inspire a new generation of “stand-off” imaging systems. These systems would allow for remote inspection for radioactive materials.

This review article intends to capture the synergy of international commercial collaborations exemplified by the United States Defense Advanced Research Projects Agency’s (DARPA’s) SIGMA program in which detector expertise originating from the United Kingdom (Kromek Group plc.) algorithm development and system modeling and analysis developed by United States national laboratories came together under the general guidance provided by a small commercial unit, Invincea Labs, in the area of network algorithm integration and development.

Keywords: Gamma detection system, Compton imaging, scintillator, semiconductor, energy resolution, contextual sensing

1. BACKGROUND

Illicit trafficking of nuclear materials is a global issue that requires monitoring and surveillance of different pathways (roadways, airways, and maritime passages) in and out of a country. International concern over nuclear terrorism has grown during the last few decades. This has driven the growth of large portal monitors and associated adjudicating system at the national border crossings. During the Cold War era the threat was primarily of nuclear weapons and its clandestine delivery methods. Proliferation and illicit trafficking of kilogram quantities of special nuclear materials was another aspect of the threat, which triggered advanced spectroscopic signature detection research of shielded and masked nuclear materials. In spite of the end of the Cold War in 1991, a new form of nuclear terrorism emerged—the demonstration of the power of dirty bombs to elicit a sense of fear, spur economic loss, and generally disrupt normal life.

Around 1990, primarily to be able to develop early warning systems in response to Chernobyl (1986)-type nuclear power plant accidents and subsequent release of large quantity of transboundary radioactive materials containing fission products and the trafficking of radioactive materials across the national borders, a number of European countries established radiation-detection systems at main border crossings, including seaports. The European Radiological Data Exchange Platform (EURDEP) [3] was created to ensure public confidence in nuclear industries by making radiation monitoring data accessible to public. It showcases for the public the large amount of radiation monitoring data gathered by these networked fixed monitoring stations. In 1994 Germany proposed at the International Atomic Energy Agency (IAEA) General Conference to control the illicit trafficking of radioactive materials at the national borders. This effort triggered the initiation of the Illicit Trafficking Radiation Assessment Program (ITRAP) in 1997. Together with United States, the European Union initiated a series of validation test series program called the Illicit Trafficking Radiation Assessment Program (ITRAP+10) for evaluation of performance of commercially available radiation detection and measurement devices [4]. The September 11, 2001 attack on the twin towers of the World Trade Center in New York, USA changed the entire landscape of counterterrorism. An entirely new United States Government entity, the U.S. Department of Homeland Security (DHS) was created. In turn, the DHS quickly created the Domestic Nuclear Detection Office (DNDO) with the mission to prevent nuclear terrorism by continuously improving capabilities to deter, detect, respond to, and attribute attacks in coordination with domestic and international partners.

This article describes the current trends in materials research and engineering for development of newer radiation detection in the form of inorganic scintillators and semiconductors. Considerable efforts have been spent in capturing the radiation search/survey monitoring data within the context of the on-scene events and situational frame. Real-time radiation monitoring data overlaid on optical imagery data and gamma source imaging techniques by Compton cameras or/and coded aperture cameras are commonplace now. Two competitive gamma imaging system are described below—one using CZT pixelated elements of different volumes (H3D Corporation) and the other uses germanium crystal (PHDS, Inc.). Both these instruments are handheld easy-to-use instruments for field work. There are also large mobile (vehicle-mounted) gamma imaging systems described below.

2. SCINTILLATORS

Demand for high-efficiency, high-resolution, fast scintillators for gamma ray detection and imaging applications is steadily rising. Focused research in growth and manufacturing of scintillators for gamma ray measurement has been driven by an increased need for scintillators with superior performance for high energy particle physics experiments as well as for medical imaging. Thanks to facilities like the Lawrence Berkeley National Laboratory High Throughput Facility for Scintillator Materials Discovery and SLYNCI (Scintillator Light-Yield Non-proportionality Characterization Instrument), it is feasible to design a scintillator for a specific purpose. The band gap can be manipulated, the energy levels and concentration of the electron-hole traps can be finely tuned, and their influence can be damped or enhanced by specific doping for optimal performance.

The ideal scintillator should have high luminous efficiency, short decay time, low afterglow, high density, short radiation length, and a luminescence spectrum that matches the photon detector response spectrum; it should also be affordable. High-density inorganic scintillators find wide applications for nuclear radiation detection in high energy physics, nuclear medicine, oil logging, nondestructive assay and inspection, and portal and mobile radiation detection systems for national security purposes. Good quality scintillators should have certain characteristics related to their density (ρ), light yield (LY), quantum efficiency (QE , incident photon to converted electron ratio), energy non-proportionality (ρ_{np}), refractive index (μ), prominent emission peak wavelength (λ_{em}), energy resolution ($R = \Delta E/E$ – full width at high maximum), decay time (τ), effective atomic number (Z_{eff}), and timing resolution. Large scintillators ($10\text{--}1000\text{ cm}^3$) at relatively low cost with low afterglow and intrinsically low background counts are some of the attractive parameters for a scintillating material. Table 1 lists scintillation properties of common gamma ray scintillators [2 and references therein].

The scintillation mechanism is a combination of at least three broad electro-optical processes comprising of (i) the interaction with incident ionizing radiation including thermalization process, (ii) charges being carried and migrated within the scintillator body and, finally, (iii) luminescence process. The interaction process involves gamma ray interaction with electrons via (i) the photoelectric effect, (ii) Compton scattering, and (iii) pair productions for a higher-energy incident gamma ray.

The incident gamma ray within the energy range between $> 10\text{ keV}$ and 10 MeV creates energetic primary electrons that ionize nearby lattice atoms by delivering energy. The energy lost in a scintillator from the ionization process is given by Bethe formula

$$-\frac{dE}{dx} = \frac{4\pi e^4 z^2}{m_e v^2} NZ \left[\ln \frac{2m_e v^2}{I \left(1 - \frac{v^2}{c^2} \right)} - \frac{v^2}{c^2} \right], \quad (1)$$

where e = electron charge, m_e = electron mass, v = particle velocity, N , Z = number density and atomic number of the atoms, and I is the average ionization potential for the atoms

The light yield of a scintillator (quantitative definition of relative brightness of a scintillator) can be defined as a function of the impinging ionizing radiation energy E_γ , quantum efficiency (QE) of the photoluminescence process, an energy transport efficiency S from the host to emission centers, and the effective energy band gap (βE_B), where β is a constant parameter dependent of scintillator, which can be written as

$$LY = \frac{E_\gamma SQE}{\beta E_B}. \quad (2)$$

Scintillator decay time (τ) determines the timing resolution for fast scintillators. The decay time is inversely related to the speed of transfer of free electron and holes from an ionization track to the emission centers and the lifetime of the luminescence state of the activator. The decay time (τ) can be mathematically defined in terms of the decay rate (Γ) of the activators and the matrix element for the dipole operator D between the final $\langle f |$ and initial states $|i\rangle$ [5]

$$\Gamma = \frac{1}{\tau} \alpha \frac{\mu}{\lambda_{em}^3} \left(\frac{\mu^2 + 2}{3} \right)^2 \sum_f |\langle f | D | i \rangle|^2. \quad (3)$$

With the above formalism of physical understanding of how scintillators work in the detection of gamma ray we list a few common scintillators below with their characteristics.

Thallium-doped Sodium Iodide Detectors: NaI:Tl scintillation crystals are the workhorses of the gamma detection industry and are used in most standard gamma spectroscopy applications due to their high light output (45,000 photons/MeV) and excellent match of their emission spectrum (at wavelength of 415 nm) to the sensitivity of photomultiplier tubes.

Barium Fluoride Detectors: BaF₂ scintillators are intrinsic scintillators and feature ultrafast sub-nanosecond UV emissions. BaF₂ scintillators are used for fast timing measurements where sub-nanosecond time resolution is required. Supported applications include positron life studies, time of flight (TOF) measurement, and positron emission tomography (PET).

Thallium-doped Cesium Iodide Detectors:

CsI:Tl scintillators are rugged, non-hygroscopic, and do not cleave. These detectors are frequently used as an alternative to NaI:Tl for a wide range of applications.

CsI:Na is a non-hygroscopic, high light output scintillator mainly used for applications where mechanical stability and good energy resolution are required.

Undoped CsI scintillators are fast, non-hygroscopic, and feature relatively low light output. A common use of undoped CsI is in physics calorimetry applications.

Calcium-doped Cerium Bromide Detectors: $\text{CeBr}_3:\text{Ca}^{2+}$ scintillation crystals are known for their high resolution, fast decay time, and low intrinsic background properties. With a background count as low as $<0.001 \text{ c/cc/s}$ in the Ac-227 complex, CeBr_3 presents a distinct advantage over other high-resolution scintillators that suffer from this intrinsic activity. Typical energy resolution for 662 keV is $\sim 4\%$ FWHM.

Cerium-doped Lanthanum Bromide Detectors: $\text{LaBr}_3:\text{Ce}$ crystals have superb gamma energy resolution. The crystals show self-activity because of the presence of trace amounts (0.09%) of naturally occurring ^{138}La in them. Typical resolution can be $<3\%$ at ^{137}Cs gamma energy.

Europium-doped Strontium Iodide Detectors: $\text{SrI}_2:\text{Eu}$ scintillators produce very high light yields and excellent non-proportionality performance over a broad range of gamma energies. $\text{SrI}_2:\text{Eu}$ crystals are inherently free of intrinsic radioactivity, resulting in a reduction of background activity. Typical energy resolution for 662 keV is $<4\%$ FWHM.

Cerium-doped Lanthanum Bromo Chloride (LBC) Detectors: $\text{LaBr}_{2.85}\text{Cl}_{0.15}:\text{Ce}$ scintillators are bright and provide an excellent gamma energy resolution of 3% FWHM at (^{137}Cs gamma energy line) 662 keV. Commercially manufactured LBC detectors are mechanically stronger than LaBr_3 and are ideal for high-resolution gamma spectroscopy applications. The crystals are hygroscopic.

Cerium-doped Cesium Lithium Yttrium Chloride (CLYC) Detectors: Because $\text{Cs}_2\text{LiYCl}_6(\text{Ce})$ scintillators combine the characteristics of medium resolution gamma ray detectors and neutron detectors in one scintillation material, they can simultaneously detect gammas and neutrons. CLYC crystals are hygroscopic and require hermetically sealed light windows to couple to a photomultiplier tube (PMT).

Cerium-doped Yttrium Aluminum Perovskite Detectors: $\text{YAP}:\text{Ce}$ scintillators are fast, mechanically robust, and provide high light output and low Z values. Applications include MHz rate x-ray spectroscopy and synchrotron physics.

Cerium-doped Cesium Lanthanum Lithium Bromo Chloride (CLLBC) Detectors: $\text{Cs}_2\text{LiLaBr}_{4.8}\text{Cl}_{1.2}:\text{Ce}$, a relatively new material, can perform both high-resolution gamma spectroscopy with 3% FWHM energy resolution for 662 keV and simultaneous neutron detection. The dual-mode material can be used for both gamma spectroscopy and neutron detection using pulse shape discrimination (PSD).

Europium-doped Calcium Fluoride Detectors: $\text{CaF}_2:\text{Eu}$ is a low-density scintillator with a high light output. Thanks to its low Z value, it is well suited for the detection of electrons (beta particles) with a high efficiency (low backscatter fraction). $\text{CaF}_2:\text{Eu}$ is also used in phoswich scintillation detectors in combination with $\text{NaI}:\text{Tl}$.

Cadmium Tungstate Detectors: CdWO_4 , is an intrinsic scintillator with a very high density and low afterglow, and it is radiation hard. Common applications include computerized tomography (CT), DC measurements of x-rays (high intensity), and photodiode readout.

Cerium-doped Lutetium Silicate (LYSO) Detectors: $\text{Lu}_{1.8}\text{Y}_{.2}\text{SiO}_5:\text{Ce}$ crystals are fast and have high density and high Z value. Applications include PET and high energy physics.

Bismuth Germanate Oxide? (BGO) Detectors: $\text{Bi}_4\text{Ge}_3\text{O}_{12}$ crystals have high physical density of 7.13 g/cm^3 and a high Z_{eff} value of 83, which makes these crystals very suited for the detection of natural radioactivity (U, Th, K), for high energy physics applications (high photo fraction), or for use compact Compton suppression spectrometers.

Bismuth-loaded Plastic Detector: Plastic scintillators with 8% by weight doping of ^{214}Bi ($Z_{\text{eff}} = 83$, high ionization energy of 7.289 eV) shows excellent gamma ray detection properties, provides a 16% FWHM resolution at 662 keV are used in gamma portal monitors [6].

Transparent Ceramic Scintillator Detectors: Cerium-doped gadolinium garnet $[(\text{Gd},\text{Y})_3(\text{Ga},\text{Al})_5\text{O}_{12}]$ GYGAG:Ce exhibits excellent light yield proportionality over usable gamma energy range, and europium-doped lutetium oxide $[\text{Lu}_2\text{O}_3:\text{Eu}]$ has very high stopping power, but it shows self-activity due to the presence of ^{176}Lu [7].

Table 1. Scintillation properties of common gamma ray sensor elements

Scintillator	Density (g/cm ³)	Radiation Length (cm)	Luminosity (photons/MeV)	Decay Time (ns)	Emission Peak Wavelength (nm)	Refractive Index	Energy Resolution (FWHM %) at 662 keV
Sodium iodide (NaI:Tl)	3.67	2.59	38,000	245	415	1.85	5.6 (best reported)–9.0
Cesium iodide (CsI:Tl)	4.51	1.86	61,000	1,220	530	1.79	5.7–10.0
Cesium iodide (CsI:Na)	4.51	1.86	43,000	690	420	1.84	7.4
Barium fluoride (BaF ₂)	4.89	2.03	10,000	650	300	1.50	11.4
Cerium bromide (CeBr ₃ :Ca ²⁺)	5.2	1.96	68,000	21	360, 380	1.9	3.2
Cerium fluoride (CeF ₃)	6.16	1.70	2,400	30	340	1.62	20.0
Bismuth germinate (BGO)	7.13	1.12	8,200	300	480	2.15	9.0–30.0
Lutetium oxyorthosilicate (LSO)	7.40	1.14	33,000	40	420	1.82	7.5 for small, >10.0 for larger crystals
Lanthanum chloride (LaCl ₃ :Ce)	3.80	2.81	50,000	25+ slow	330, 352	1.90	3.1%
Lanthanum bromide (LaBr ₃ :Ce)	5.10	1.88	75,000	30	375	1.90	2.7–3.2
Strontium iodide (SrI ₂ :Eu)	4.55	1.95	115,000	1,200	435	2.19	2.8
Lutetium iodide (LuI ₃ :Ce)	5.60	1.70	115,000	28	470, 525	1.70	3.3
Lutetium silicate (LYSO)	7.10	1.14	27,000	30	425	1.82	12.4
RGB (RbGd ₂ Br ₇ :Ce)	4.80	1.85	56,000	43	410	—	4.1
Yttrium aluminum perovskite (YAP)	5.35	2.70	21,600	27	347	1.94	4.4
Tellurium-doped zinc selenium (ZnSe:Te)	5.42	—	55,000	50,000	645	2.67	5.4
Lead tungstate (PbWO ₄)	8.28	0.9	400	10	420	2.2	23

3. SEMICONDUCTORS

A good quality semiconductor device to be used as a gamma energy spectrometer should have certain fundamental properties intrinsic to the semiconductor materials. It should have a wide band gap energy to minimize thermal excitations of the charged carriers to populate the conduction band. The materials should have high effective atomic number Z_{eff} to provide enhanced gamma ray electron interaction within the semiconductor device volume. The ideal semiconductor material should have high atomic density, long charge-carrier lifetimes, high resistivity, high electron and hole mobilities, and a small ionization energy. A wide band gap energy (~2 eV) and high resistivity (~1010 ohm-cm) allow room-temperature operation. Materials like high-purity germanium (HPGe) have a low band gap energy of 0.67 eV, which requires cooling to avoid the electron transport to the conduction band at room temperature. HPGe, cooled by liquid nitrogen, operates at 77 K and has excellent gamma energy resolution (0.15% at ⁶⁰Co peak energy of 1332 keV); however, electro-mechanically cooled HPGe, operating at

~120 K, has somewhat worse resolution. Long charge-carrier lifetimes and high carrier mobilities increase the charge collection efficiency and produce better spectroscopic results—the product of mobility ($\mu_{e/h}$) and the lifetime ($\tau_{e/h}$) of the majority carrier (electron or hole) is a measure of the quality of a semiconductor. For CZT the electron mobility is lifetime product ($\mu\tau$)_e is about 7.5×10^{-3} cm²/V). A lower value of the pair creation energy produces larger numbers of excited electron-hole pairs, thereby improving statistics and enhancing spectroscopic energy resolution. Physical properties of some of the modern room-temperature semiconductor detectors (RTSDs) are listed in Table 2.

An excellent review article on RTSDs for nuclear security [8] was published recently in which electronic properties of candidate RTSDs were tabulated. For most of the semiconductors more electron-hole pairs are created per unit incident gamma ray energy than the number of photons created in a common scintillator. The average energy to create an electron-hole pair in a semiconductor is linearly related to the band gap energy E_B (in eV) as follows $\epsilon_{e-h} = 2.73E_B + 0.55$. With a band gap energy of 1.57 eV the most common room-temperature semiconductor, CZT, will have a pair creation energy of about 4.8 eV. From a 1 MeV gamma ray the number of electron-hole pairs created in CZT will be more than 200,000, whereas in the most commonly used scintillator, namely NaI:Tl, there are only 38,000 photons created per MeV of gamma ray energy. The number of information carrying quanta (electron-hole pairs) produced in semiconductor and (photons) created in scintillators from an incident gamma ray is closely related to the full width half-maximum resolution of the detection devices. If we assume the formation of charge carriers or photons are governed by a Poisson statistical process, the fractional resolution due to a purely Poisson process can be given by

$$R = \frac{2.35}{\sqrt{N}}, \quad (4)$$

where N is the number of information carrying quanta. In the literature an additional factor called Fano Factor (F) is introduced to correct for the dispersion of a probability distribution, defined as

$$F = \frac{\text{Observed variance in } N}{\text{Poisson variance in } N}. \quad (5)$$

The statistical component of the resolution becomes

$$R = 2.35 \sqrt{\frac{F}{N}}. \quad (6)$$

This explains why the resolution of a NaI:Tl scintillator is 25 to 32 times worse than that of a germanium detector.

4. STUDIES OF NOVEL SEMICONDUCTORS

We are pursuing a three-year tiered research project to experimentally study the efficacy of an inexpensive cesium lead bromide (CsPbBr₃) semiconductor that has gamma ray detection property in bulk superior to the current industry standard of CZT. In nanocrystalline configuration the material has high power conversion efficiency (~22%) as a solar cell. Nanocrystals with a fluorescence quantum yield of 77% have been achieved. Theoretical studies based on the density functional theory (DFT) formalism will be made to explain, understand, and exploit the remarkably high carrier mobilities, large diffusion lengths, and fault tolerance through testing the concept of large polaron formation.

The best room-temperature semiconductor, pixelated CZT, is expensive (\$2K/cm³) and still hard to grow in sizes greater than 1 cm³. Cesium lead bromide, a direct wide band gap (2.3 eV) semiconductor, can be grown from the melt in large sizes inexpensively (\$3/cm³) and provides gamma energy resolution (3.8% FWHM at 662 keV) in planar mode using asymmetric electrodes (Ga-Au). The low impurity in crystals (10 ppm for 69 elements), high effective atomic number (65.9 compared to 50.2 for CZT), the high lifetime (τ) and mobility lifetime (mt) parameters for holes respectively 25 mS and 1.34×10^{-3} cm² V⁻¹, make CsPbBr₃ a superior semiconductor.

Working with crystal manufacturing companies like Saint Gobain Corp. and Radiation Monitoring Devices, Inc., CsPbBr₃ crystal samples in bulk (~10 cm³), nanocrystalline form, and pixelated sizes (for imaging purposes) will be procured to benchmark the carrier mobility, fault tolerance, and opto-electronic properties. Properties affecting the sensitivity (cps/mSvh⁻¹), gamma energy resolution (% FWHM) at a given incident gamma energy, and radiation hardness will be characterized by choosing the best asymmetric electrode pairs and detector dimensions.

Results from research, and analysis on optimized wet processes to grow nanosheets from colloidal solutions with special attention to reduction of the labile nature CsPbBr₃, will be reported. Opto-electronic properties, like power conversion efficiency as solar cells and work function (WF, the thermodynamic energy to create electron-hole pairs from semiconductor surface) of the semiconductor will be benchmarked. It is expected that CsPbBr₃ will

Table 2. Properties of semiconductors used in gamma ray detectors and measurements at room temperature

Material	Atomic Number	Density ρ (g/cm ³)	Band Gap (eV)	E_{pair} (eV)	Resistivity ($\Omega\text{-cm}$)	$\mu\tau$ (e) Product (cm ² /V)	$\mu\tau$ (h) Product (cm ² /V)
Silicon (Si)	14	2.33	1.12	3.62	10^4	>1	~1
Germanium (Ge)	32	5.33	0.67	2.96	50	>1	>1
4H silicon carbide (4H-SiC)	14, 6	3.20	2.20	9.00 (est.)	> 10^5	4×10^{-4}	8×10^{-5}
Gallium arsenide (GaAs)	31, 33	5.32	1.43	4.20	10^7	8×10^{-5}	4×10^{-6}
Indium phosphide (InP)	49, 15	4.78	1.35	4.20	10^7	4.8×10^{-6}	$<1.5 \times 10^{-5}$
Cadmium selenide (CdSe)	48, 34	5.81	1.73	5.5	10^6	6.3×10^{-5}	7.5×10^{-5}
Cadmium telluride (CdTe)	48, 52	5.85	1.44	4.43	10^9	3.3×10^{-3}	2×10^{-4}
Cadmium zinc telluride (Cd _x Zn _(1-x) Te)	48, 30, 52	~6.00	1.50–2.20	5.00	10^{11}	1×10^{-3}	6×10^{-6}
Lead iodide (PbI ₂)	82, 53	6.20	2.32	4.90	10^{12}	8×10^{-6}	3×10^{-7}
Mercuric iodide (HgI ₂)	80, 53	6.40	2.13	4.20	10^{13}	10^{-4}	4×10^{-5}
Thallium bromide (TlBr)	81, 35	7.56	2.68	6.50	10^{12}	1.6×10^{-5}	1.5×10^{-6}
Mercuric bromo iodide (HgBrI)	80, 35, 53	6.20	2.40–3.40	—	5×10^{13}	1×10^{-6}	$<1 \times 10^{-7}$
Cadmium telluride selenide (CdTe _{0.5} Se _{0.5})	48, 52, 34	5.81	1.47	4.56	5×10^9	4×10^{-3}	—
Mercuric selenide iodide (Hg ₃ Se ₂ I ₂)	80, 34, 53	—	2.12	6.34	1.2×10^{12}	1.0×10^{-5}	—
Indium iodide (InI)	49, 53	—	2.00	6.01	1×10^{11}	7×10^{-5}	—
Thallium mercuric iodide (Tl ₄ HgI ₆)	52, 80, 53	—	—	—	$10^{11} - 10^{12}$	8×10^{-4}	—
Cadmium manganese telluride (CdMnTe)	48, 25, 52	5.8	1.61	2.12	2×10^{10}	7×10^{-3}	—

provide 182,000 electron-hole pairs (assuming a WF of 5.5 eV) compared to 38,000 photons per MeV of incident gamma ray energy from NaI:Tl, which makes the semiconductor's gamma energy resolution approximately 2.2 times better than that from NaI:Tl. Working with solid-state theoretical physicists from Sandia National Laboratories with massive computational power, using DFT formalism, the WF, valence band minimum (with optimized sublayers like NiPt) of CsPbBr₃ will be benchmarked, and the power conversion efficiency of the semiconductor as solar cell will be optimized.

One minor risk is that most of the manufacturing facilities growing CsPbBr₃ are in China. The commercial viability of this semiconductor as solar cells will increase the interests of U.S. manufacturing companies to grow the crystals in bulk, in polycrystalline form and as nanocrystals.

Large (comparable to NaI:Tl logs that are $2'' \times 4'' \times 16''$) CsPbBr_3 single crystals with asymmetric electrodes can be designed to provide a high sensitivity (similar to NaI:Tl) and resolution (comparable to CZT) gamma ray detection system at the cost of polyvinyl toluene (PVT) plastic. Use of the crystals in pixelated form may result in higher gamma energy resolution than CZT, thereby providing a better gamma ray imaging system. It is envisioned that the solar cells (in nanocrystalline form) may provide the power required to run a large single-crystal planar diode, making it a self-sustained gamma ray detection system.

5. GAMMA RAY IMAGING

Gamma ray imaging is the nondestructive technique and process of creating visual representations of a point or distributed gamma-emitting materials that are not easily accessible or viewable by the naked eye. The technique of gamma ray imaging has been applied in nuclear physics, astronomy, medical diagnostics, national security, and nuclear power industries. Gamma ray imaging techniques for static and dynamic gamma source localization and visualization within a cargo or shielded or masked traffic of materials (like on a conveyor belt) have widespread tactical applications for the law enforcement and emergency response organizations. Fast (less than 2 minutes) gamma ray images superimposed on optical images of the container for millicurie amounts of a gamma-emitting source could bring a long, labor-intensive radiation search process to a successful stop. Conventional gamma ray imagers use Compton cameras or coded aperture cameras. Hybrid cameras using Compton and coded aperture techniques simultaneously for large vehicle-mounted systems [Standoff Radiation Detectors (SORDs)] [9] capable of imaging gamma sources at distances ranging from 10 to 100 meters have been developed by DHS.

Two commercial vendors, namely H3D Corporation (Ann Arbor, Michigan) and PHDS, Inc. (Knoxville, Tennessee) have manufactured gamma ray imagers for practical use by first responders and power plant surveyors. The H3D imager uses a Polaris [10] series of 3D, position-sensitive, pixelated CZT semiconductor elements of different volumes ranging from 4.5 to $>19 \text{ cm}^3$, all with an excellent gamma energy resolution of $<1.1\%$ FWHM at a reference gamma energy of ^{137}Cs (662 keV) to develop fast-acting (fewer than 2 minutes start-up time), dependable, portable gamma imaging systems that are finding industrial applications in nuclear power plants, safeguarding, and national security. Progress has been made since the original concept of applying 3D, position-sensitive, pixelated CZT in the area of materials development, detector mounting, electronic readout ASICs, event reconstruction algorithm, calibration procedures, and noise reduction techniques to imaging.

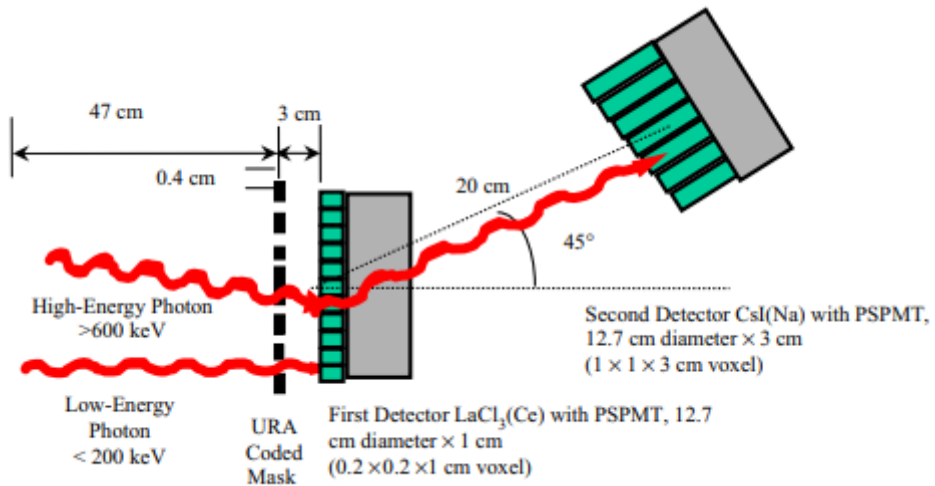


Figure 1. Pictorial description of Compton and coded aperture hybrid gamma ray imaging camera [11]

PHDS, Inc. manufactures the germanium gamma ray imaging (GeGI) detector system, which has very high gamma ray energy resolution (0.3% FWHM at 662 keV), large field of view (360°), and takes advantage of an optical imaging camera. It is lightweight (6.8 kg) and can be hand carried or put on an auto pan-tilt tripod stand. The system is very fast in response and claims to identify $10 \mu\text{Ci}$ of ^{137}Cs at 1 meter within 3.7 ± 1 sec. [12] The wide-angle optical camera combined with a gamma ray imaging spectrometer can depict the nuclear environment rapidly and accurately. Using Compton imaging overlaid with optical images, the GeGI performs very well at close range and excels at the detection of targets at large distances. GeGI has been designed with an electro-mechanical cooler so there is no need for liquid nitrogen cooling. This feature makes the device lighter than comparable detection systems. Figure 2 shows a GeGI system with the laptop display.



Figure 2. GeGI, PHDS' germanium gamma ray imaging system

The congressional justification of the DHS CWMD budget overview for fiscal year 2019 emphasizes the Nuclear and Radiological Imaging Platform (NRIP) and urges that the platform leverage recent advancements in the commercial sector as well as prior transformational research and development work done by the department. The goal, through combining passive and active technologies, is to develop new imaging devices in a single system to provide real-time gamma ray images of nuclear and radiological threat objects regardless of the amount of shielding or the complexity of the cargo. Stresses are put on developing newer electronics, sensor fusion, and advanced software algorithms for analytics. The Airborne Radiological Enhanced-sensor System (ARES) technology facilitates radioactive materials search by enabling fusion of radiation detection with other sensing modalities (e.g., multispectral imaging, GPS, altimetry, etc.) [13]

6. PROPOSED WORK ON CONTEXTUAL SENSORS

Contextual sensing is a current concept in which intelligent sensor systems are deployed and the data collected from them are cleverly juxtaposed and curated in a way that emulates how a human senses an accident area by implementing a smart data fusion architecture. It automatically opens up the system to machine data learning and artificial intelligence applications. The concept of data fusion from contextual sensors along with radiation measurement devices is best exemplified in biomedical imaging where images from positron emission tomography (PET) and single photon emission computer tomography (SPECT) are fused with x-rays, ultrasound, and magnetic resonance imaging (MRI) images for improved diagnosis and localization of abnormal tissues.

The Remote Sensing Laboratory has undertaken research projects to enhance collection, compilation, and curation of multisensory real-time data for radiological search, localization, and identification of radioactive materials for tactical responses. Four major areas of enhancement are being investigated, including incorporation of (i) gated gamma imagery system (turns on only in high-dose areas), (ii) video imagery in GPS-denied areas to create a 2D map using inertial measuring unit, (iii) x-ray imagery system with an analysis tool for shielding characterization around the target materials, and (iv) detectors for precursor airborne contamination. Rigorous customized data fusion architecture to capture the scenario description is being designed.

Currently each component of data obtained from the field to create a seamless event description is executed separately in a time-ordered manner. Sequential deployment of gross gamma count device, gamma spectrometer, gamma imagery cameras, x-ray devices to collect data, and subsequent analysis make the process lengthy and usually not amenable to smart curation. The proposed architecture is a choreographed organization of sensors, data acquisition, and processing techniques supported by a fusion architecture. The fusion architecture creates a composite view of observations and captures additional circumstantial information that cannot be obtained using individual sensors.

At a minimum, the deployable system will include (i) a high sensitivity plastic gamma ray gross count/dose rate detector, (ii) a CZT-based gamma spectroscopy system, (iii) a pixelated CZT gamma imaging system, and (iv) a Gold-150 x-ray imagery system with XTK tool kit software and a static/video optical imaging camera. Use of a

CsPbBr_3 semiconductor (proposed in the section titled: STUDIES OF NOVEL SEMICONDUCTORS may combine operations (i) through (iii) effectively. Application of small form factor iCAM (Intelligent Continuous Air Monitor) manufactured by Mirion Technologies, Inc. for environmental monitoring to discern trace airborne contamination is envisioned. Considerable work in data stream management is expected. A large-bandwidth secured data communication link to the Home Team for triage support to the incident will be required.

Smart curation of multisensory data will provide seamless time evolution of complex radiological or nuclear incidents. The data fusion architecture will lend itself to accept ubiquitous sensory data if available and applicable. The integrated system will drastically cut down the response time and can also be deployed very easily from multiple platforms like drones and all-terrain vehicles (ATVs) and robots.

7. CONCLUSION

Intensive research and development work in academic and commercial circles is developing application-specific scintillation devices for medical imaging, space physics, and high energy physics activities. Measured trade-offs are being made between stopping power, resolution, and decay constants of scintillation materials to achieve the desired engineering goals. Commercial development of specialized gamma detection systems powered by university and national laboratory-level research has become commonplace. Understanding of non-proportionality of scintillation light yield with varying incident gamma energy is being facilitated by the Scintillator Light Yield Non-proportionality Characterization Instrument (SLYNCI) [14] at Lawrence Berkeley National Laboratory. In the area of semiconductors, growth technique enhancement, purification of crystals, sizes of grown crystals, and the associated costs are still issues to be solved. A few inorganic and hybrid organic-inorganic perovskite compounds like CsPbBr_3 , MAPbI_3 (methyl ammonium lead iodide) have shown high mobility lifetime product ($>10^{-2} \text{ cm}^3/\text{V}$) in single crystals to be effective as room-temperature semiconductor devices. The advantage of hybrid semiconductors is that they can be grown large in size from solutions at a relatively low temperature.

REFERENCES

- [1] Department of Homeland Security, “Intelligent Radiation Sensing System,” (23 August 2019). <https://www.dhs.gov/intelligent-radiation-sensing-system>
- [2] Milbrath, B. D., Peurrung, A. J., Bliss, M., and Weber, W. J., “Radiation detector materials: An overview,” J. Mater. Res. 23(10), 2561-2581 (2008). <https://doi.org/10.1557/JMR.2008.0319>
- [3] EU Science Hub, “EUropean Radiological Data Exchange Platform,” <https://ec.europa.eu/jrc/en/publication/european-radiological-data-exchange-platform>
- [4] EU Science Hub, “Illicit Trafficking Radiation Assessment Program (ITRAP+10) Test campaign summary report,” <https://ec.europa.eu/jrc/en/publication/illicit-trafficking-radiation-assessment-program-itrap10-test-campaign-summary-report>
- [5] Yanagida, T., “Inorganic scintillating materials and scintillation detectors,” Proc. Japan Academy, Series B – Physical and Biological Sciences 94(2), 75–97 (2018). <https://www.ncbi.nlm.nih.gov/pmc/articles/PMC5843761/>
- [6] Cherepy, N. J., Hok, S., O’Neal, S. P., Martinez, H. P., Beck, P. R., Sanner, R. D., Drury, O. B., Swanberg, E. L., Payne, S. A., and Hurlbut, C. R., “Bismuth-loaded plastic scintillator portal monitors,” Proc. SPIE 10762, 107620B (2018). <https://doi.org/10.1117/12.2320884>
- [7] Cherepy, N., Kuntz, J., Seeley, Z., Fisher, S., Drury, O., Sturm, B., Hurst, T., Roberts, J., and Payne, S., “Transparent ceramic scintillators for gamma-ray spectroscopy and radiography,” Proc. SPIE August (2010). <https://www.researchgate.net/publication/252188037>
- [8] Johns, P. M. and Nino, J. C., “Room temperature semiconductor detectors for nuclear security,” J. Appl. Phys. 126, 040902 (2019). <https://doi.org/10.1063/1.5091805>
- [9] Department of Homeland Security, System Assessment and verification for Emergency Responders (SAVER), “Standoff Radiation Detectors,” https://www.dhs.gov/sites/default/files/publications/SRDs-TN_1212-508_0.pdf.
- [10] Wahl, C. G., Kaye, W. R., Wang, W., Zhang, F., Jaworski, J. M., King, A., Boucher, Y. A., and He, Z., “The Polaris-H imaging spectrometer,” Nucl. Instrum. Methods Phys. Res. A 784(1), 377-381 (2015).

[11] Lee, W. and Wehe, D. "Hybrid gamma ray imaging—Model and results," Nucl. Instrum. Methods Phys. Res. A 579, 200-204 (2007). <https://doi.org/10.1016/j.nima.2007.04.039>

[12] Southern Scientific, GeGI Rad Nuc Standoff Detector (19 December 2019). <https://www.southernscientific.co.uk/products-by-manufacturer/phds-co/gegi>

[13] Department of Homeland Security Countering Weapons of Mass Destruction Budget Overview (21 January 2020). <https://www.dhs.gov/sites/default/files/publications/CWMD%20FY19%20CJ.pdf>

[14] Choong, W-S., Hull, G., Moses, W. W., Vetter, K. M., Payne, J. A. Narine Cherepy, J., and Valentine, J. D., "Performance of a Facility for Measuring Scintillator Non-proportionality," (2008). <https://escholarship.org/content/qt6341r5vx/qt6341r5vx.pdf>

ACKNOWLEDGMENT

This manuscript has been authored by Mission Support and Test Services, LLC, under Contract No. DE-NA0003624 with the U.S. Department of Energy, National Nuclear Security Administration, NA-10 USDOE NA Office of Defense Programs (NA-10). The United States Government retains and the publisher, by accepting the article for publication, acknowledges that the United States Government retains a non-exclusive, paid-up, irrevocable, worldwide license to publish or reproduce the published form of this manuscript, or allow others to do so, for United States Government purposes. The U.S. Department of Energy will provide public access to these results of federally sponsored research in accordance with the DOE Public Access Plan (<http://energy.gov/downloads/doe-public-access-plan>). The views expressed in the article do not necessarily represent the views of the U.S. Department of Energy or the United States Government. DOE/NV/03624--0792.